Computational design of metamorphic In(N)AsSb mid-infrared light-emitting diodes

Reza Arkani[1,2,*], Christopher A. Broderick[1,2], and Eoin P. O'Reilly[1,2]
[1]Tyndall National Institute, Lee Maltings, Dyke Parade, Cork T12 R5CP, Ireland
[2]Department of Physics, University College Cork, Cork T12 YN60, Ireland
[*]Email: r.arkani@umail.ucc.ie

***Abstract*—We present a theoretical investigation of the optical properties of metamorphic $InN_y(As_{1-x}Sb_x)_{1-y}/Al_zIn_{1-z}As$ type-I quantum wells (QWs) designed to emit at mid-infrared wavelengths. The use of $Al_zIn_{1-z}As$ metamorphic buffer layers has recently been demonstrated to enable growth of lattice-mismatched $InAs_{1-x}Sb_x$ QWs having emission wavelengths $\gtrsim 3$ μm on GaAs substrates. However, little information is available regarding the properties of this newly established platform. We undertake a theoretical analysis and optimisation of the properties and performance of strain-balanced structures designed to emit at 3.3 and 4.2 μm, where we recommend the incorporation of dilute concentrations of nitrogen (N) to achieve emission beyond 4 μm. We quantify the calculated trends in the optical properties, as well as the ability to engineer and optimise the overall QW performance. Our results highlight the potential of metamorphic $InN_y(As_{1-x}Sb_x)_{1-y}/Al_zIn_{1-z}As$ QWs for the development of mid-infrared light-emitting diodes, and provide guidelines for the growth of optimised structures.**

I. Introduction

Mid-infrared light-emitting diodes (LEDs) and lasers operating in the first atmospheric window, at wavelengths between 3 and 5 μm, are of importance for a range of practical applications: e.g. detection of trace gases, atmospheric pollutants or biological markers in chemical process control and non-invasive medical diagnostics, as well as applications in free-space optical communications [1]. Within this spectral range, wavelengths close to 3.3 and 4.2 μm – at which the greenhouse gases CH_4 (methane) and CO_2 (carbon dioxide) respectively possess strong absorption features – are of particular interest for applications in environmental monitoring [2], [3].

Mid-infrared LEDs and lasers are typically grown on relatively expensive GaSb or InAs substrates, which are less technologically mature compared to the GaAs- and InP-based platforms commonly employed in near-infrared optical communications. Existing devices operating in the 3 – 5 μm spectral range are generally limited by optical and electrical losses, which are in part associated either with the use of (i) type-I quantum wells (QWs) having relatively low band offsets, in which case thermal carrier leakage limits performance at and above room temperature, or (ii) type-II QWs or superlattices based on $InAs_{1-x}Sb_x$ and related alloys, which possess intrinsically low optical efficiency compared to type-I structures. It has recently been demonstrated that growth on $Al_zIn_{1-z}As$ metamorphic buffer layers (MBLs) provides a potential route to overcome these limitations, by facilitating the growth of QWs having large type-I band offsets, thereby delivering high optical efficiency and suppressed thermal leakage [4].

Here, we present a theoretical analysis and optimisation of the properties and performance of metamorphic $InN_y(As_{1-x}Sb_x)_{1-y}/Al_zIn_{1-z}As$ QWs designed to emit at 3.3 and 4.2 μm. We quantify the design space made available using these QWs and demonstrate that (i) 3.3 μm emission can be readily achieved in strain-balanced structures having large type-I band offsets, and (ii) the QW structural properties can be engineered to enhance the spontaneous emission (SE) at a desired emission wavelength. We identify that optimum performance can be achieved in structures possessing tensile strained $Al_zIn_{1-z}As$ barriers. The strain-balanced structures we consider have the potential to mitigate issues related both to carrier confinement and strain-thickness limitations, thereby enabling growth of multi-QW or superlattice structures having high structural quality. Our analysis indicates that while ternary $InAs_{1-x}Sb_x/Al_zIn_{1-z}As$ QWs are constrained to emission wavelengths $\lesssim 4$ μm, incorporation of nitrogen (N) in $InN_y(As_{1-x}Sb_x)_{1-y}/Al_zIn_{1-z}As$ dilute nitride QWs can be used to extend the emission wavelength out to 4.2 μm.

II. Theoretical model

Our theoretical model of the electronic and optical properties of $InN_y(As_{1-x}Sb_x)_{1-y}/Al_zIn_{1-z}As$ metamorphic QWs is based on a 10-band **k·p** Hamiltonian for the $InN_y(As_{1-x}Sb_x)_{1-y}$ band structure. This model includes the conventional (8-band) set of conduction and valence band (CB and VB) edge zone-centre Bloch basis states, augmented by the inclusion of a (spin-degenerate) N localised state [5]. The coupling between the N localised and $InAs_{1-x}Sb_{1-x}$ (host matrix) extended CB edge states is described via a band-anticrossing interaction. The N-related parameters of the 10-band Hamiltonian have been explicitly computed via atomistic electronic structure calculations, and provide a quantitative description of the evolution of the main features of the band structure with N composition y [6].

Our numerical (envelope function) **k·p** calculation of the QW eigenstates proceeds via a reciprocal space plane wave expansion method, which provides a robust and efficient framework within which to compute and analyse the electronic and optical properties [7]. Key to our analysis is the direct use of the QW eigenstates in the calculation of the SE spectra, meaning that important band mixing and localisation effects associated with N incorporation, epitaxial strain and quantum confinement are accounted for explicitly. We analyse the performance of candidate QW structures for LED applications by computing the radiative current density at fixed temperature ($T = 300$ K) and injected sheet density ($n_{2D} = 10^{11}$ cm^{-2}). Optimised structures are identified by maximising the SE rate at the desired emission wavelength. Full details of the theoretical model, as well as the parameters used in our calculations, can be found in Ref. [8].

III. RESULTS

Here, we provide an overview of the results of our theoretical design and analysis of $InN_y(As_{1-x}Sb_x)_{1-y}/Al_zIn_{1-z}As$ strain-balanced QWs, grown on relaxed $Al_{0.125}In_{0.875}As$ MBLs and desiged to emit at 3.3 and 4.2 μm. Firstly, in Sec. III-A we describe the procedure we have established to design strain-balanced structures having a specified emission wavelength. Then, in Sec. III-B, we provide a summary of the calculated trends in the optical properties of these structures, and comment on routes to achieve optimised structures for practical applications in mid-infrared LEDs. Full details of our analysis will be presented in Ref. [8].

A. Design of strain-balanced QW structures

We have firstly used our theoretical model to identify the ranges of strain and band gap (emission wavelength) accessible to pseudomorphically strained bulk-like $InN_y(As_{1-x}Sb_x)_{1-y}$ alloys grown on $Al_{0.125}In_{0.875}As$ MBLs. The results of this analysis are summarised in Fig. 1(a), where dashed and solid lines respectively denote paths in the composition space along which the in-plane strain ϵ_{xx} and band gap are constant. Firstly, we find that for growth on an $Al_{0.125}In_{0.875}As$ MBL, which has a lower lattice constant than that of InAs (the latter corresponding in Fig. 1(a) to $x = y = 0$), pseudomorphically grown $InN_y(As_{1-x}Sb_x)_{1-y}$ alloys are in a state of compressive strain ($\epsilon_{xx} < 0$). Secondly, we note that incorporation of Sb in N-free ($y = 0$) alloys leads to a rapid decrease of the band gap with increasing x, allowing access to mid-infrared emission wavelengths. Specifically, we calculate that a band gap of 0.3 eV – corresponding to an emission wavelength ≈ 4.1 μm – can be achieved in a compressively strained $InAs_{1-x}Sb_x/Al_{0.125}In_{0.875}As$ alloy having $x = 7.5\%$.

Incorporation of N simultaneously reduces the band gap and lattice constant [6], allowing longer emission wavelengths to be achieved at fixed ϵ_{xx} than in a N-free alloy. Quaternary $InN_y(As_{1-x}Sb_x)_{1-y}$ alloys therefore offer a route to achieve long emission wavelengths while circumventing strain-thickness limitations. We calculate that a band gap of 0.3 eV can be achieved in $InN_y(As_{1-x}Sb_x)_{1-y}/Al_{0.125}In_{0.875}As$, at a compressive strain of 1.0%, for Sb and N compositions $x = 4.5\%$ and $y = 0.7\%$. Overall, these calculations demonstrate that 3 – 5 μm emission wavelengths can be readily achieved at Sb and N compositions, and compressive strains, compatible with established epitaxial growth [4].

Having described the general features of the bulk band stucture of $InN_y(As_{1-x}Sb_x)_{1-y}/Al_{0.125}In_{0.875}As$, we turn our attention now to the design of $InN_y(As_{1-x}Sb_x)_{1-y}/Al_zIn_{1-z}As$ QWs grown on $Al_{0.125}In_{0.875}As$ MBLs to target (i) strain-balanced structures, and (ii) fixed 3.3 and 4.2 μm emission wavelengths. We begin by noting that the calculations presented in Fig. 1(a) are for bulk-like alloys. To design a QW structure having a given emission wavelength then requires that the Sb and N compositions x and y be increased, in order to compensate for the confinement energy of the bound electron and hole states (which is typically ~ 50 – 100 meV). To target 3.3 μm (0.376 eV) emission we consider N-free ($y = 0$) structures, while to target 4.2 μm (0.295 eV) emission we consider N-containing QWs, where we find that incorporation of dilute N compositions ($y \lesssim 4\%$) can be used to bring about the additional band gap reduction necessary to push the emission wavelength out to and beyond 4 μm. Next, we note that since the $InN_y(As_{1-x}Sb_x)_{1-y}$ alloys described by Fig. 1(a) are compressively strained, growth of strain-balanced structures requires the use of tensile strained $Al_zIn_{1-z}As$ barrier layers (i.e. barrier layers having $z > 12.5\%$).

We identify strain-balanced structures by requiring that each QW-barrier repeat has zero net in-plane stress. Imposing this condition allows the derivation of a relationship linking the ratio of the in-plane strains $\epsilon_{xx,w}$ and $\epsilon_{xx,b}$ in the QW and barrier layers to the ratio of the corresponding layer thicknesses t_w and t_b [9]:

$$\frac{\epsilon_{xx,b}}{\epsilon_{xx,w}} = -\frac{A_w\, a_b\, t_w}{A_b\, a_w\, t_b}\,, \tag{1}$$

where a denotes the lattice constant, $A = C_{11} + C_{12} - 2C_{12}C_{11}^{-1}$ is determined by the elastic constants C_{11} and C_{12}, and the subscripts w and b respectively denote the QW and barrier layers.

To design strain-balanced QWs emitting at 3.3 μm we proceed as follows. Firstly, we define the ratio between the thicknesses t_w and t_b of the QW and barrier layers. For the analysis presented here we set $t_b = 3\,t_w$, which is kept fixed for all calculations. Secondly, for a chosen QW thickness t_w we select a "test" QW Sb composition x, which determines the QW lattice constant a_w, in-plane strain $\epsilon_{xx,w}$ and elastic parameter A_w. Thirdly, the barrier Al composition z is varied, to identify the barrier lattice constant a_b, in-plane strain $\epsilon_{xx,b}$ and elastic parameter A_b satisfying Eq. (1). For a given choice of QW thickness t_w and Sb composition x, solving Eq. (1) in this manner then identifies the barrier Al composition z required to ensure overall strain-balancing. Fourthly, having a strain-balanced structure we perform a full numerical calculation of the electronic and optical properties (cf. Sec. II), employing a strain-balanced calculational supercell of total length $L = t_w + t_b$. Finally, this procedure is repeated as a function of the "test" QW Sb composition x, to determine the composition at which the calculated peak of the room temperature SE spectrum is at 3.3 μm. For a given choice of t_w this procedure then identifies the QW Sb composition x and barrier Al composition z producing 3.3 μm emission from a strain-balanced QW.

Detailed analysis indicates that it is difficult to extend the emission wavelength of $InAs_{1-x}Sb_x/Al_zIn_{1-z}As$ structures grown on $Al_{0.125}In_{0.875}As$ MBLs to $\gtrsim 4$ μm, due to a combination of issues related to carrier confinement and strain-thickness limitations [4]. We therefore propose that – for a fixed MBL Al composition – emission wavelengths $\gtrsim 4$ μm can be achieved by utilising $InN_y(As_{1-x}Sb_x)_{1-y}$ dilute nitride QWs. To target 4.2 μm emission we consider strain-balanced $InN_y(As_{1-x}Sb_x)_{1-y}/Al_zIn_{1-z}As$ structures. The procedure we follow to design these structures is as outlined above for the N-free 3.3 μm structures, but is modified to account for the fact that use of a quaternary QW enables the band gap and in-plane strain to be selected independently of one another (cf. Fig. 1(a)). For each QW Sb composition x we choose the N composition y such that $\epsilon_{xx,w} = -1.5\%$. That is, at 4.2 μm we consider QWs having variable thickness t_w and a fixed compressive strain of 1.5%.

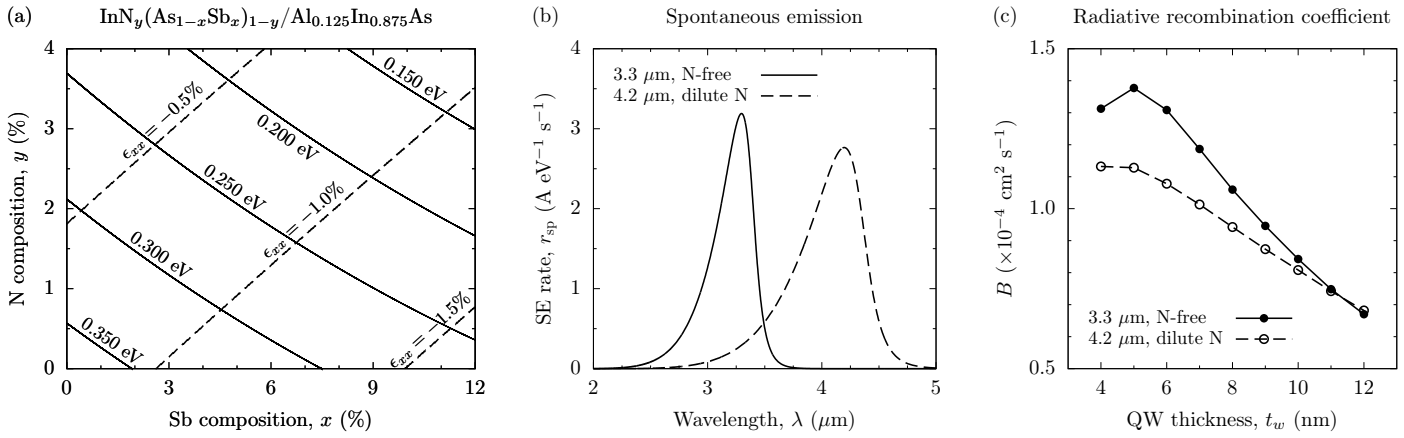

Fig. 1. (a) Composition space map illustrating the ranges of in-plane strain (ϵ_{xx}) and room temperature band gap (or, equivalently, emission wavelength) assessible using pesudomorphically strained $InN_y(As_{1-x}Sb_x)_{1-y}$ bulk-like epitaxial layers grown on an $Al_{0.125}In_{0.875}As$ MBL. Dashed and solid lines respectively denote paths in the composition space along which ϵ_{xx} and the emission wavelength are constant. (b) Calculated room temperature SE spectra, at fixed sheet carrier density $n_{2D} = 10^{11}$ cm^{-2}, for strain-balanced structures having $t_w = 8$ nm and designed to emit at 3.3 μm (N-free; solid line) and 4.2 μm (dilute nitride; dashed line). (c) Calculated variation of the radiative recombination coefficient B with QW thickness t_w for strain-balanced structures designed to emit at 3.3 μm (N-free; closed circles) and 4.2 μm (dilute nitride; open circles). The 4.2 μm structures have fixed compressive strain $\epsilon_{xx,w} = -1.5\%$.

B. Strain-balanced QWs at 3.3 and 4.2 μm: optical properties

Having identified strain-balanced structures emitting at 3.3 and 4.2 μm, we compute here the electronic and optical properties of these structures as a function of the QW thickness t_w. This enables us to (i) elucidate and quantify general trends in their radiative (spontaneous) emission rate, as well as to (ii) identify optimised structures suitable for epitaxial growth and experimental investigation. We quantify the former by calculating the SE spectrum at fixed sheet carrier density ($n_{2D} = 10^{11}$ cm^{-2}), from which we compute the radiative current density J_{rad} and radiative recombination coefficient B. In this manner our analysis identifies the ranges of alloy composition, epitaxial strain and layer thicknesses which maximise the SE rate, thereby specifying strain-balanced QWs which can be expected to optimise LED performance.

To target 3.3 μm emission we focus on N-free ($y = 0$) $InAs_{1-x}Sb_x/Al_zIn_{1-z}As$ QWs, and consider structures having QW thicknesses ranging from $t_w = 4$ – 12 nm. Following the procedure outlined in Sec. III-A we find that narrow QWs require relatively high Sb compositions x to achieve 3.3 μm emission, but that the required Sb composition decreases significantly with increasing t_w. At $t_w = 4$ nm we calculate that an Sb composition $x = 17.5\%$ is required to achieve 3.3 μm emission, with a correspondingly high barrier Al composition $z = 20.8\%$ required to achieve strain balancing. As t_w is increased to 12 nm we calculate that to maintain 3.3 μm emission the QW Sb composition is reduced to $x = 4.9\%$, with a barrier Al composition $z = 17.5\%$ required to maintain strain balancing.

The solid line in Fig. 1(b) shows the calculated SE spectrum for the structure having $t_w = 8$ nm, in which the QW Sb and barrier Al compositions are $x = 8.3\%$ and $z = 18.5\%$. We note that the presence of type-I band offsets in these QWs leads to good overall radiative efficiency: the calculated ground state (inter-band) optical transition matrix element has a relatively high value of 18.41 eV, which in turn produces a high calculated peak SE rate $r_{sp,max} = 3.2$ A eV^{-1} s^{-1} at 3.3 μm [4]. Integrating the SE spectrum we compute $J_{rad} = 170$ mA cm^{-2} for this structure. Then, writing $J_{rad} = eBn_{2D}^2$ in the Boltzmann approximation, we extract the radiative recombination coefficient $B = 1.06 \times 10^{-4}$ cm^2 s^{-1} at $T = 300$ K which, e.g., exceeds by a factor of approximately two that calculated for a comparable InP-based dilute bismide QW structure designed to emit at 3.5 μm [10]. The closed circles in Fig. 1(c) show the variation of B with t_w calculated in this manner – i.e. at fixed sheet carrier density n_{2D} for structures having the same emission wavelength. We find that B is maximised for $t_w = 5$ nm, at which thickness we calculate $B = 1.38 \times 10^{-4}$ cm^2 s^{-1}, indicating that the SE rate is maximised in narrow QWs.

Turning our attention to structures designed to emit at 4.2 μm, we focus on $InN_y(As_{1-x}Sb_x)_{1-y}$ QWs having fixed compressive strain $\epsilon_{xx,w} = -1.5\%$. For a narrow QW having $t_w = 4$ nm we find that relatively high QW Sb and N compositions $x = 18.2\%$ and $y = 3.0\%$ are required to achieve 4.2 μm emission. As t_w is increased to 12 nm, we calculate that the required Sb and N compositions are significantly reduced, to $x = 11.8\%$ and $y = 0.7\%$. Since these structures have fixed $\epsilon_{xx,w}$, the barrier Al composition required to achieve strain balancing is effectively independent of t_w (cf. Eq. (1)): we calculate $z = 19.0\%$ to within 0.1% for 4 nm $\leq t_w \leq$ 12 nm.

The dashed line in Fig. 1(b) shows the calculated SE spectrum at $n_{2D} = 10^{11}$ cm^{-2} for the structure having $t_w = 8$ nm, in which the QW Sb and N compositions are $x = 13.3\%$ and $y = 1.2\%$. Firstly, we note that the peak SE rate, $r_{sp,max} = 2.8$ A eV^{-1} s^{-1} at 4.2 μm, for this dilute nitride structure is approximately 13% lower than that calculated for the equivalent N-free structure designed to emit at 3.3 μm (cf. solid line in Fig. 1(b)). This reduction in the peak SE rate is expected to arise for the structures considered due to a combination of (i) the reduction in band gap in going from a 3.3 to 4.2 μm emission wavelength, and (ii) a reduction in the ground state optical transition matrix element, associated with the impact of N-related band-anticrossing on the calculated QW CB edge eigenstates [5], [8]. However, for the dilute nitride structure having $t_w = 8$ nm we calculate that the ground

state optical transition matrix element is approximately 95% of that calculated for the equivalent N-free structure designed to emit at 3.3 μm. This suggests that the primary factor leading to reduced SE rate in the dilute nitride structures at fixed t_w is the emission wavelength since, at fixed temperature and sheet carrier density, the SE rate is directly proportional to the band gap [5].

Integrating the SE spectrum for this structure gives $J_{\text{rad}} = 151$ mA cm^{-2}, from which we extract $B = 0.94 \times 10^{-4}$ cm^2 s^{-1}. Repeating this analysis as a function of t_w we again calculate that B, and hence the SE rate, is maximised for narrow QWs having $t_w = 4$ – 5 nm, at which thickness we calculate $B = 1.13 \times 10^{-4}$ cm^2 s^{-1}. The results of these calculations – which are depicted using open circles in Fig. 1(c) – suggest that, for $t_w \gtrsim 10$ nm, the radiative efficiency in an ideal dilute nitride QW designed to emit at 4.2 μm should be approximately equal to that of a N-free structure designed to emit at 3.3 μm. We note however that, in practice, the radiative efficiency of dilute nitride structures is likely to be somewhat reduced, due to challenges associated with the growth of N-containing alloys having high material quality.

The calculated trends in the SE for both the 3.3 and 4.2 μm structures indicate that the radiative efficiency is maximised for narrow QWs, $t_w \approx 5$ nm. However, the Sb and N compositions x and y required to achieve a fixed emission wavelength are higher in narrower QWs, due to the requirement to compensate the larger carrier confinement energies in such structures. Similarly, larger QW Sb compositions x mandate higher barrier Al compositions z in order to achieve strain-balancing, making strain-thickness limitations of concern for the growth of the relatively thick barrier layers. The difficulty associated with incorporating Sb and/or N while maintaining high material quality during epitaxial growth then favours the growth of thicker QWs, which require lower x and y (and correspondingly, lower z in the barrier layers). Overall, our analysis therefore identifies a trade-off of key practical importance for the growth and fabrication of LEDs based on these novel heterostructures.

IV. Conclusion

We have presented a theoretical investigation and optimisation of the optical properties of 3.3 and 4.2 μm $\text{InN}_y(\text{As}_{1-x}\text{Sb}_x)_{1-y}$ QWs grown on $\text{Al}_{0.125}\text{In}_{0.875}\text{As}$ MBLs. By quantifying the scope offered by this material system to undertake strain and band structure engineering we demonstrated that there is large scope for the design of QW structures, incorporating compressively strained quaternary $\text{InN}_y(\text{As}_{1-x}\text{Sb}_x)_{1-y}$ QWs having unstrained or tensile strained ternary $\text{Al}_z\text{In}_{1-z}\text{As}$ barriers. Such QWs combine large type-I band offsets with emission wavelengths $\gtrsim 3.3$ μm – offering the possibility to design devices having high optical efficiency and reduced temperature sensitivity – making these structures particularly appealing for the development of mid-infrared LEDs.

We have defined design criteria to achieve strain-balanced QWs at a desired emission wavelength, thereby providing a general method which can be applied to produce candidate multi-QW or superlattice structures for epitaxial growth and experimental investigation. Our analysis indicates that emission wavelengths $\lesssim 4$ μm can be achieved in N-free structures, making $\text{InAs}_{1-x}\text{Sb}_x/\text{Al}_z\text{In}_{1-z}\text{As}$ QWs of particular interest for practical applications at 3.3 μm. To achieve emission at wavelengths beyond 4 μm we found that it was necessary to utilise dilute nitride $\text{InN}_y(\text{As}_{1-x}\text{Sb}_x)_{1-y}$ QWs in order to circumvent issues related to carrier confinement and strain-thickness limitations. Specifically, we demonstrated that N compositions $y \lesssim 3\%$ are sufficient to achieve emission at 4.2 μm in strain-balanced structures.

Via a systematic analysis of strain-balanced structures designed to emit at 3.3 and 4.2 μm we identified key trends in their properties and performance as functions of alloy composition, QW thickness and epitaxial strain. Overall, our analysis confirms the promise of these novel metamorphic heterostructures for the development of high-performance mid-infrared LEDs, and provides guidelines for the growth of optimised devices suitable for practical applications.

Acknowledgment

This work was supported by the European Commission via the Marie Skłodowska-Curie Innovative Training Network PROMIS (project no. 641899), by Science Foundation Ireland (SFI; project no. 15/IA/3082), and by the National University of Ireland (NUI; via the Post-Doctoral Fellowship in the Sciences, held by C.A.B.). The authors thank Ms. Eva Repiso, Mr. James A. Keen, Dr. Peter J. Carrington, and Prof. Anthony Krier (Lancaster University, UK) for useful discussions.

References

[1] A. Krier, Ed., *Mid-Infrared Semiconductor Optoelectronics*. Springer, 2007.

[2] J. Hodgkinson and R. P. Tatam, "Optical gas sensing: a review," *Meas. Sci. Technol.*, vol. 24, p. 012004, 2013.

[3] D. Jung, S. Bank, M. L. Lee, and D. Wasserman, "Next-generation mid-infrared sources," *J. Opt.*, vol. 19, p. 123001, 2017.

[4] E. Repiso, C. A. Broderick, R. Arkani, E. P. O'Reilly, P. J. Carrington, and A. Krier, "Optical properties of metamorphic type-I $\text{InAs}_{1-x}\text{Sb}_x/\text{Al}_y\text{In}_{1-y}\text{As}$ quantum wells grown on GaAs for the mid-infrared spectral range," *submitted*, 2018.

[5] S. Tomić, E. P. O'Reilly, R. Fehse, S. J. Sweeney, A. R. Adams, A. D. Andreev, S. A. Choulis, T. J. C. Hosea, and H. Riechert, "Theoretical and experimental analysis of 1.3-μm InGaAsN/GaAs lasers," *IEEE J. Sel. Topics Quantum Electron.*, vol. 9, p. 1228, 2003.

[6] E. P. O'Reilly, A. Lindsay, P. J. Klar, A. Polimeni, and M. Capizzi, "Trends in the electronic structure of dilute nitride alloys," *Semicond. Sci. Technol.*, vol. 24, p. 033001, 2009.

[7] M. Ehrhardt and T. Koprucki, Eds., *Multiband Effective Mass Approximations: Advanced Mathematical Models and Numerical Techniques*. Springer, 2014.

[8] R. Arkani, C. A. Broderick, and E. P. O'Reilly, "Theory and design of strain-balanced In(N)AsSb/AlInAs metamorphic quantum wells for applications in mid-infrared light-emitting diodes," *submitted*, 2018.

[9] N. J. Ekins-Daukes, K. Kawaguchi, and J. Zhang, "Strain-balancing criteria for multiple quantum well structures and its signature in x-ray rocking curves," *Cryst. Growth Des.*, vol. 2, p. 287, 2002.

[10] C. A. Broderick, W. Xiong, S. J. Sweeney, E. P. O'Reilly, and J. M. Rorison, "Theory and design of $\text{In}_x\text{Ga}_{1-x}\text{As}_{1-y}\text{Bi}_y$ mid-infrared semiconductor lasers: type-I quantum wells for emission beyond 3 μm on InP substrates," *in press*, 2018.